Environmental Science Advances

Accepted Manuscript

This article can be cited before page numbers have been issued, to do this please use: V. Ettler, M. Mihaljevi, T. Zadorova, D. Žížala, A. Vank, V. Penížek, B. Kíbek, O. Sracek and B. Mapani, *Environ. Sci.: Adv.*, 2026, DOI: 10.1039/D6VA00064A.

ROYAL SOCIETY OF CHEMISTRY

rsc.li/esadvances

Research paper submitted to Environmental Science: Advances
(VA-ART-02-2026-000064.R2, revised version June 2026)

View Article Online
DOI: 10.1039/D6VA00064A

Wildland fire impacts on temporal and spatial patterns of trace elements in smelter-affected semiarid soils

Vojtěch Ettler[1]*, Martin Mihaljevič[1], Tereza Zádorová[2], Daniel Žížala[3], Aleš Vaněk[2], Vít Penížek[2], Bohdan Kříbek[4], Ondra Sracek[5] & Ben Mapani[6]

1. Institute of Geochemistry, Mineralogy and Mineral Resources, Faculty of Science, Charles University, Albertov 6, 128 00 Prague 2, Czech Republic (*corresponding author, E-mail: ettler@natur.cuni.cz)

2. Department of Soil Science and Soil Protection, Faculty of Agrobiology, Food and Natural Resources, Czech University of Life Sciences Prague, Kamýcká 129, 165 00 Prague 6, Czech Republic

3. Remote Sensing and Pedometrics Laboratory, Research Institute for Soil and Water Conservation, Žabovřeská 250, 156 00 Prague 5, Czech Republic

4. Czech Geological Survey, Geologická 6, 152 00 Prague 5, Czech Republic

5. Department of Geology, Faculty of Science, Palacký University in Olomouc, 17. listopadu 12, 771 46 Olomouc, Czech Republic

6. Department of Civil, Mining and Process Engineering, Namibia University of Science and Technology, Windhoek, Namibia

ORCID numbers:
Vojtěch Ettler (https://orcid.org/0000-0002-0151-0024)
Martin Mihaljevič (https://orcid.org/0000-0002-4875-9345)
Tereza Zádorová (https://orcid.org/0000-0002-5541-2155)
Daniel Žížala (https://orcid.org/0000-0002-7685-7604)
Aleš Vaněk (https://orcid.org/0000-0002-6156-3419)
Vít Penížek (https://orcid.org/0000-0001-6131-7608)
Bohdan Kříbek (https://orcid.org/0000-0002-8095-9363)
Ondra Sracek (https://orcid.org/0000-0002-3085-6358)
Ben Mapani (https://orcid.org/0000-0002-5354-3397)

View Article Online
DOI: 10.1039/D6VA00064A

Environmental significance

A chronosequence of smelter-impacted vegetation-soil interfaces from areas affected by wildland fires in 2012, 2021, and 2023 in northern Namibia indicated moderate contamination levels. The role of legacy lead mining and the ongoing smelting of arsenic-bearing copper ores in shaping the spatial distribution patterns of trace elements was highlighted. A fire-induced increase in the soil pH may enhance the downward migration of arsenic and other trace elements in the soil profiles. High arsenic leaching from litter and topsoils, exceeding the water quality guidelines, could represent a potential risk for local water resources during its mobilization with the first rainfall of the wet season.

Abstract

Wildland fires affect the trace element cycles at the vegetation-soil interface. We studied the trace elements (As, Cd, Co, Cr, Cu, Hg, Ni, Pb, Sb, V, Zn) patterns in grass, litter, and soils located near a non-ferrous metal smelter in semiarid Namibia, collected along a chronosequence of fire events occurring in 2012, 2021, and 2023. The soils are not excessively contaminated, but the Pb isotopic analysis confirmed that the legacy mining and smelting are responsible for the metal(loid)s dispersion in the studied area. Comparisons of unburned and burned plots indicated that changes in trace element concentrations were most pronounced in litter and topsoil. The ash color, changes in the trace element concentrations, and their enrichment factors suggest that the fires in the area were of low intensity with temperatures <400 °C. Whereas Hg, and to a lesser extent also As, were partly re-emitted back to the atmosphere, other smelter-derived contaminants concentrated in the ash. The high leaching of As observed in the litter and topsoils (up to 233 µg/L) exceeds water quality guidelines and may be further enhanced by a fire-induced increase in soil pH. Our findings suggest that even moderately contaminated environments in the semiarid savanna, which are vulnerable to burning during the dry period, pose a potential risk to local water resources by mobilizing contaminants following the first rainfall of the wet season.

View Article Online
DOI: 10.1039/D6VA00064A

Introduction

Non-ferrous metal smelters are key sources of soil contamination[1] and the contamination of aboveground vegetation.[2,3] Review studies indicate particularly elevated concentrations of many inorganic contaminants in soils in the vicinity of non-ferrous smelters, such as metals (Cd, Co, Cu, Ni, Pb, Zn) or metalloids (As, Sb), reflecting the chemical compositions of the processed ore concentrate and the main extracted metals in a given metallurgical operation.[1,4,5] The spatial distribution of contamination around smelters is dependent on prevailing winds and the size of the dust emissions. Contaminants associated with mining operations are generally coarser-grained than the smelter-derived ones, which are often concentrated in the ultrafine aerosol particle fractions (< 0.5 μm) and may travel to greater distances.[1,4] Although most metals/metalloids are generally deposited in areas adjacent to smelters[1,3,4], several studies have demonstrated that smelter-derived contamination may be observed tens of km away.[6,7] The highest levels of contaminants in smelter-affected soils are generally found in the surface soil horizons, but partial downward movement of metals and metalloids in the soil profiles *via* leaching, or other processes, was also documented at numerous sites.[1,8]

With the increasing frequency and severity of wildland fires[9,10] and the occurrence of fires at the wildland-urban interface[11], highly polluted areas in the proximity of mines and smelters, especially in semiarid or subtropical regions, can also be affected by fires.[12-14] Our previous soil survey in a mining district in Zambia revealed that, despite the expected high interception of smelter-derived aerosols by the tree canopies, surprisingly high metal concentrations were found in the grasslands compared to wooded plots.[8] It was suggested that more extensive bushfires in forested areas could be the reason for the lower metal concentrations in the forest litter due to re-emissions.[8,15]

View Article Online
DOI: 10.1039/D6VA00064A

Field studies demonstrated that Hg is substantially volatilized[16-19], and experiments confirmed that Hg re-emissions back to the atmosphere occur at relatively low temperatures (~340 °C).[20] Based on the literature survey, the behavior of other trace elements is much less straightforward.[21,22] It is generally assumed that the temperature-dependent transformation of organic matter during the burning should lead to an increase in concentrations of most trace elements in the burned soil and ash compared to the unburned soils.[11,23] However, such changes are not observed at all sites and they are likely not directly related to the fire severity[24], and exhibit a temporal evolution after a fire event.[23] As an example, Abraham et al.[12] studied contaminated soils before and after the controlled burn in a former mining area and found that As, Cd, Ni, and Zn increased in the post-burn soil, whereas Hg, Cr, and Pb decreased; however, only Hg, Mn, and Zn showed a statistically significant difference. A follow-up study[13] demonstrated that the mobility of trace elements in the soil increased immediately after the fire, probably due to soil enrichment with ash particles; in the long term (3-12 months), the trace elements' mobility decreased due to ash removal by wind, rainfall, and leaching. The term "mobilization" of trace elements after the fire is often unclear in many fire-related studies; it may either correspond to a temperature-induced re-emission[25-27], wind transport of trace elements-bearing aerosols[28] or fine ash particles back to the atmosphere[29], an increase in "plant-available" species in soils likely caused by a change in the solid-phase or redox speciation[30,31] or a release into water bodies causing the subsequent contamination of drinking water reservoirs, vastly studied in many post-fire areas.[32-35]

To better understand the effects of fire on trace elements in soil systems, a need for more systematic studies of the vertical and lateral variations in toxic substances has recently been identified.[22] Because most fires heat only the uppermost centimeters of the soil[36], many previous studies focused only on the litter and/or ash layers, and the investigation into the depth-related migration of pollutants in the fire-affected surface soil horizons remains very

View Article Online
DOI: 10.1039/D6VA00064A

rare in the literature.[22] To fill this gap, this article aims to expand our understanding of the effects of fire on the trace element patterns at the vegetation-litter-topsoil-subsoil interface in the semiarid savanna, which is affected by non-ferrous metal mining and smelting activities. We studied plots situated near the Tsumeb copper smelter in northern Namibia, representing a chronosequence from freshly burned areas to sites 11 years post-fire. The specific objectives were: (i) to characterize the depth-related and spatial patterns of trace elements using multi-element chemical analyses; (ii) to use Pb isotopes for the determination of the sources and the fate of Pb in the local fire-affected soil environments, and (iii) to assess the risk of the release of trace elements from the burned soil with water extractions and aqueous speciation modeling.

Experimental

Study area

The Tsumeb area is situated in the Otavi Mountainland of the Oshikoto region in northern Namibia (Fig. 1). Tsumeb is a renowned mining city with over 100 years of mining and ore-processing history.[37] The Tsumeb ore body, a polymetallic pipe-like deposit formed within the carbonate rocks (predominantly Otavi dolomite) containing Cu, Pb, Zn, As, Sb, Cd, Co, Ge, Ga, Hg, Mo, Ni, Sn, W, and V was in operation between 1906-1998; it produced more than 27 Mt of ore, yielding approximately 1.9 Mt of Cu, 3 Mt of Pb, and 1 Mt of Zn, as well as Ag, Ge, As and Sb as by-products.[37,38] The Cu and Pb smelters, processing local ores, were in operation in Tsumeb from 1907; the smelting technology evolved, and after the closure of the Tsumeb mine, the Pb smelter was dismantled in the 2010s while the Cu smelter still operates and processes Cu concentrates from abroad (at the time of sampling, the Canadian company Dundee Precious Metals Tsumeb operated the smelter, but the operation was sold to

View Article Online
DOI: 10.1039/D6VA00064A

the Chinese company Sinomine in 2024).[20,39,40] Another ore extraction operation in the studied area is Tschudi, located approximately 20 km west of Tsumeb.[37] It consists of disseminated Cu-Ag sulfidic mineralization occurring in sandstones, mined in the years 1996–1997, followed by steady production from 2015 to 2020, when heap leaching and electrowinning were adopted.[37,41]

Prevailing easterly winds (ESE, E, ENE) are responsible for the dust and related contamination dispersion in the area. The contamination hotspot is thus located westerly of the smelter and the nearby mine tailings facilities and metallurgical dumps, which are considered the most critical source of contamination by metals and metalloids (mainly As, Cu, and Pb) (Fig. S1).[3] This has been confirmed by many previous studies focusing on the spatial distribution and sources of metal(loid) contaminants in the vegetation and soils in the Tsumeb area.[2,3,20,42,43]

The Tsumeb area experiences a hot semiarid climate (BSh according to the Köppen-Geiger climate classification) with a mean annual temperature of 23.3 °C (23.7 °C in 2023, the year of sampling) and a mean annual precipitation of 534 mm (335 mm in 2023) with extremely seasonal distribution, falling between October/November and March/April (https://www.MeteoBlue.com). The dominant trees and (dwarf) shrub species in the study area are *Acacia* sp., *Boscia albitrunca/foetida* (shepherd's tree/bush), *Albizia anthelminica* (worm-cure albizia), *Dichrostrachys cinerea* (sicklebush), *Grewia flava* (brandy bush), and *Tarchonanthus camphorathus* (camphor bush). The main grass species are *Eragrostis porosa* (thalia lovegrass) and *Aristida stipitata* (long-awned three-awn) (Figs S2 and S3). The soil cover of the wider Tsumeb area is dominated by the Calcisols reference soil group with the frequent presence of petrocalcic horizons[43] and weakly developed Leptosols on the rock outcrops. Regosols occur mainly on the younger sedimentary cover. Patches of more developed Cambisols and Luvisols occur in the southern part of the area.[44] The soil A-

View Article Online
DOI: 10.1039/D6VA00064A

horizons, being the most relevant for our study, are generally developed down to a depth of 20 cm.[45,46]

Sampling and processing of solid materials

A preliminary selection of sampling locations was based on wildfire outbreak dates using NASA FIRMS (Fire Information for Resource Management System), which has provided information on wildfire occurrence and duration since 2000. The exact area affected by the wildfire was then delineated at the pre-selected locations using satellite imagery from the Landsat 7 ETM+ (1999–2024) and Sentinel-2 (2015–present) sensors. Time series of false-color images (SWIR, NIR, and red bands combined) were used to identify fires, which were then verified locally using the Normalized Burn Ratio (NBR) time series. Two sites near Tsumeb, where wildland fires occurred in 2012 and 2021, were selected according to the following criteria: (i) they have experienced no fire since they were burned; (ii) they are situated downwind of the Tsumeb mine/smelter area (i.e., in the presumable direction of the airborne contamination); (iii) they are accessible (i.e., not on the private land) (Fig. S4a,b). Moreover, during the 2023 field campaign, another fire event occurred upwind, but closer to the town of Tsumeb (~6 km southeast) (Fig. S4c). Here, we collected samples 3 weeks after the fire from both burned and unburned areas to obtain comparative reference materials. Nevertheless, the satellite imagery indicated that this spot also experienced fires in the past, especially during the 2012 fire season (Fig. S4a).

Despite the rapid recovery of the bush vegetation after the fire (Fig. S2a), the field survey revealed signs of past fire activity in the area, including burned acacia trunks (Fig. S2b), ash layers, and char fragments (Fig. S2c-e). The 2023 “running fire” mainly affected the grass, acacia bushes, and litter (Figs S2c and S3).

View Article Online
DOI: 10.1039/D6VA00064A

At each site, samples were collected at three spots using a plastic shovel (Fiskars, Finland). For soil collection at each site, we used the modified EuroGeoSurvey methodology, using a 2 × 2 m grid to collect five subsamples (in each corner and the center of the square) to obtain one composite sample.[48] We collected grass samples (if available, n = 8), litter (n = 12), and two layers of the surface soil horizon A: uppermost soil (denoted, for practical reasons, as "topsoil", depth: 0-1 cm; n = 12), and deeper soil (denoted hereafter as "subsoil", depth: > 1 cm, generally 1-5 cm; n = 12). Given that fires affect only the uppermost soil layers[36], the deeper soil horizons were not sampled. When possible, rock fragments corresponding to the local geological background (exclusively carbonates in the studied area) were also collected either in the outcrops or in the deeper soil horizons (> 30 cm) to obtain material for the bulk chemical and Pb isotopic analysis (n = 5). The GPS coordinates and basic descriptions of the sampled areas are reported in Table S1.

The soils and biomass samples were air-dried. The soil and litter samples were sieved to 2 mm using a stainless-steel sieve (Retsch, Germany). The bedrock was manually crushed by a geological hammer. Aliquots of the litter, soils, and rocks were further pulverized in an agate mortar (Retsch planetary mill PM 400, Germany). Grass samples were pulverized in a cutting mill (Fritsch Pulverisette 14, Germany). The fine powders of all the samples were further used for digestion and the subsequent determination of the total elemental and Pb isotopic compositions, as well as for the color determination on the dry samples using Munsell® soil color charts.

The digestion procedures varied according to the matrices analyzed. For soil or biomass samples, 0.2 g was decomposed using a hot acid mixture (9 ml of concentrated HNO_3 and 3 ml of concentrated HF; Merck Ultrapure, Germany) in a microwave unit (Multiwave 5000, Anton Paar, Austria). The dissolved sample was transferred into polytetrafluoroethylene (PTFE) beakers (Savillex, USA) and evaporated on a hot plate. The solution residuum was

View Article Online
DOI: 10.1039/D6VA00064A

dissolved in 2% HNO_3 (v/v) and used for the subsequent chemical analysis. The carbonate bedrocks were digested in closed PTFE beakers: 0.2 g of solid was dissolved in 3 ml of concentrated HNO_3 for 1 h at 120 °C on a hot plate; subsequently 5 ml of concentrated HF and 0.5 ml of concentrated $HClO_4$ were added, evaporated to near dryness, re-dissolved in 100 ml of 2% HNO_3 (v/v) and used for the subsequent chemical analysis. Moreover, to obtain the Pb isotopic signatures of the Tsumeb copper smelter emissions, the previously studied flue dust samples collected in the flue gas cleaning system of the smelter (n = 4)[49,50] were digested using the following procedure: 0.02 g of sample was dissolved in closed PTFE beakers in 3 ml of a 3:1 mixture of concentrated HNO_3 and HCl (called inverted or Lefort *aqua regia*), for 24 h on a hot plate; subsequently 2 ml of concentrated HF was added, evaporated to near dryness, re-dissolved in 50 ml of 4% HNO_3 (v/v), diluted and used for the subsequent chemical and isotopic analysis.

Physicochemical, elemental, and Pb isotopic analyses

The soil pH was measured in deionized water according to the ISO 10390 method (1:5 solid-to-liquid ratio, with 5 minutes of vigorous agitation followed by 2 hours of decantation).[51] A WTW Multi 3620 IDS pH meter, equipped with a WTW Sentix 940 pH electrode, was calibrated against WTW technical buffers 4.01 and 7.00 (WTW, Germany).

The total organic and inorganic carbon (C_{org} and C_{inorg}) and total sulfur (S_{tot}) in the pulverized soil and biomass samples were determined using a combination of ELTRA CS 530 and ELTRA CS 500 TIC analyzers (ELTRA, Germany). The pulverized samples were also used to analyze total mercury (Hg) using a Leco-Altec AMA 254 atomic absorption spectrometer. The soil, biomass, and bedrock digests were analyzed for the total concentrations of As, Cd, Co, Cr, Cu, Ni, Pb, Sb, Ti, V, and Zn using a quadrupole-based inductively coupled plasma

View Article Online
DOI: 10.1039/D6VA00064A

mass spectrometry (ICP-MS; Thermo Scientific iCAP-Q™; Thermo Scientific, Germany) operating under standard analytical conditions. The same instrument, equipped with a Peltier-cooled (~2 °C) cyclonic spray chamber and a Meinhard-type nebulizer, was used for determining the Pb isotopic composition ($^{206}Pb/^{207}Pb$ and $^{208}Pb/^{206}Pb$ ratios). For the Pb isotopic measurements, all samples and reference materials were diluted with 2% (v/v) HNO_3 to concentrations of 10–20 µg/L Pb to achieve optimal sensitivity. A correction for the mass bias was performed using a calibrator-sample bracketing method with a common lead (NIST SRM 981) isotopic standard.

Soil leaching in water

To assess the water-soluble concentrations of the trace elements from the litter and soils, we used the United States Geological Survey (USGS) fast leaching test according to the methodology of Hageman[52], which has been adopted for a variety of geomaterials, including forest-fire-burned soils. The solid sample (sieved to < 2 mm and pulverized) was placed in falcon vials and leached in deionized water at a liquid-to-solid ratio of 20 (0.5 g soil into 10 ml of solution), intensively shaken for 5 minutes on a horizontal shaker (GLF 3018, Germany, 150 reverses/min), then allowed to settle for 10 min. The vials with the suspensions were centrifuged (Hettich Universal 320 R, Germany; 3500 RPM, 3 min). The original method states that pH and electrical conductivity (EC) are measured directly in the suspension, and another subsample is taken after filtering the leachate for chemical analysis.[52] We tested the pH and conductivity measurements on both the unfiltered and filtered samples and found excellent agreement between the two measurements ($R^2 = 0.9525$ for the pH and $R^2 = 0.9867$ for the EC); for this reason, the physicochemical parameters were measured in the filtered subsamples only. The aliquot parts of the extracts were filtered using disposable

View Article Online
DOI: 10.1039/D6VA00064A

0.45-µm membrane filters (Millex LCR, Millipore, USA) connected to 20-mL syringes (B-Braun, Germany).

The pH and redox potential values in the water leachates were measured using a WTW Multi 3620 IDS multimeter equipped with a Sentix 940 pH electrode and a SenTix® ORP-T900 redox electrode (Xylem Inc., USA), respectively. The instrument was calibrated against WTW technical buffers with pH levels of 4.01 and 7.00, as well as a WTW RH28 redox standard solution (220 mV at 25 °C). The electrical conductivity (EC) of the leachates was measured using a Mettler-Toledo Seven2Go conductometer equipped with a Mettler-Toledo InLab® 738 ISM conductivity probe (Mettler-Toledo, Switzerland). The trace and selected major elements in the extracts (Al, As, Ca, Cd, Co, Cr, Cu, Fe, K, Mg, Mn, Na, Ni, Pb, Sb, Ti, V, and Zn), necessary for subsequent geochemical modeling, were determined using an inductively coupled plasma mass spectrometer (ICP-MS) with collision cell and MS/MS separation (Agilent 8900 Triple Quad, USA).

Quality control/quality assurance and data processing

The quality control/quality assurance (QC/QA) procedure was carried out by the parallel digestion and analysis of soil standard reference materials SRM 2709a (San Joaquin Soil) and SRM 2711a (Montana II Soil) released by the National Institute of Standards and Technology (NIST, USA) and a rock certified reference material BCR-2 (Columbia River Basalt) released by the United States Geological Survey (USGS). The latter certified reference material was also used to verify the Pb isotopic measurements. Moreover, a NIST SRM 1463f reference material (Trace elements in water) was repeatedly analyzed to verify the accuracy of the ICP measurements in the digests and water extracts (Table S2).

View Article Online
DOI: 10.1039/D6VA00064A

The obtained data were processed and plotted using a combination of the Prism 11 for Mac (GraphPad, USA) and Graphic for Mac (Picta, USA) software packages. Prism 11 was also used for the statistical data treatment. The normality of data was assessed using the Shapiro-Wilk test (alpha = 0.05). A one-way or two-way analysis of variance (ANOVA) and Tukey's multiple comparison test (alpha = 0.05) was performed to evaluate the statistical differences between the individual chemical parameters of the samples from the burned and unburned areas. To understand correlations among water-extracted trace elements, soil properties, and total trace element concentration, a correlation matrix with nonparametric Spearman correlation coefficients was calculated ($P < 0.05$).

To better assess the fate of trace elements during the fire, normalization to relatively conservative, lithogenic elements (also used as natural dust tracers in the atmospheric sciences), such as Fe, Al, or Ti, is often performed.[53,54] For our samples from the burned and unburned plots from the 2023 event, the concentrations of the measured metals/metalloids (Me) were normalized to Ti, expressed as Me/Ti ratios. Subsequently, to assess the enrichment of a given trace element in a sample ($[Me/Ti]_{sample}$) with respect to the natural background ($[Me/Ti]_{bedrock}$) and to compare the depletion or enrichment of the samples during the fire, we calculated the enrichment factors (EFs) as follows:

$$EF = \frac{[Me/Ti]_{sample}}{[Me/Ti]_{bedrock}}$$

The geochemical code PHREEQC-3 for Mac[55] was used for the speciation-solubility calculations to determine the speciation of trace elements in the leachates and to calculate the degree of leachate saturation with respect to the potential solubility-controlling phases, as indicated by the saturation index (SI). For all the calculations, we used the minteq.v4.dat

View Article Online
DOI: 10.1039/D6VA00064A

thermodynamic database, and the data below the limit of detection (LOD) were entered into the code as the LOD values.

Results and discussion

Basic soil properties

Despite visible signs of past fire activity at plots burned 11 and 2 years before sampling (e.g., Fig. S2b), the development of a newly formed layer of litter at both sites indicates rapid ecosystem recovery. Except for the charcoal layer, forming a topsoil layer at one of the three sampled plots burned in 2021, no color indications of ash presence were observed in the soil (Table S3; Fig. S5). However, substantial differences in color were observed for the unburned and burned litter for the 2023 fire event, with changes from grayish brown to very dark gray (5YR 3/1) or even black (10YR 2/1) in the ash layer (Table S3; Fig. S5).

The C_{org} content varies across soil profiles (Fig. 2a; Table S4) and differences between the individual layers are statistically significant ($P < 0.004$). Whereas the aboveground grass biomass samples have very similar C_{org} concentrations (around a median value of 42.7 wt%), the highest variability in C_{org} was found for the litter, the layer the most affected by the fire (5.82–40.5 wt%, median: 26.5 wt%) (Table S4; Fig. 2a). This variability reflects the loss of organic matter during the fire, most visible when the unburned litter and ash layer from the 2023 fire event are compared; the median C_{org} decreased from 14.3 to 7.8 wt.% (Table S4; Fig. 2b). Previous experimental studies showed that fire leads to significant carbon losses.[19] Badía et al.[56] reported a carbon loss of ~50% in fire-affected dry soil and ~25% in wet soil, and our results are in perfect agreement with this finding. The formation of a charcoal layer in one of the plots burned in 2021 (C_{org}: 60 wt.%) indicates that a pyrolytic burning of wooded biomass occurred at this spot, likely at a higher temperature and under the conditions

View Article Online
DOI: 10.1039/D6VA00064A

of a smoldering fire.[57,58] This pyrogenic carbon corresponds to a recalcitrant form of C_{org} and its biodegradation is a very slow process[59] compared to the much faster degradation of the uncharred ash formed by the rapid burning of grass and litter.[58] Based on the color determination of our samples (see above), we assume the latter fire regime occurred at most of the studied plots with the dominant grass and shrubland vegetation with temperatures corresponding to a low intensity fire (<400 °C)[60,61] (Figs 1 and S2). Interestingly, although the soils are developed on carbonate rocks, relatively low concentrations of C_{inorg} were determined in all the samples (<0.01 to 2.66 wt%). This is probably due to the intensive sedimentary transport (fluvial, aeolian and colluvial) over relatively long distances. The upper part of the soil profile is therefore often separated from the in-situ weathered rock by a lithic discontinuity.[47]

The pH varied in the range of 5.8–7.9 for the litter (median: 6.5) and 6.9–8.5 for the topsoil/subsoil (median: 8.1) (Fig. 3a; Table S4). In agreement with the literature data[33], a comparison of the unburned litter and the resulting ash of the 2023 fire event shows a statistically significant increase in pH (from 6.7 ± 0.46 to 7.8 ± 0.04; $P < 0.011$, one-way ANOVA, Tukey's multiple comparison test) (Fig. 3b).

Trace element distribution and leaching patterns, and related fire effects

The trace element distributions in the vegetation, soil profiles, and bedrocks are depicted in Fig. 3 and reported in Table 1 (basic statistics) and Table S4 (whole dataset). Table 1 also presents the median reference values for the area near the Tsumeb smelter, where Kříbek et al.[3] and Tuhý et al.[20] investigated the spatial distribution of metal(loid) contaminants in the vegetation and soils. Globally, the total trace element concentrations in our samples are below or close to these reference median values (Table 1). Moreover, a comparison with the

View Article Online
DOI: 10.1039/D6VA00064A

Canadian Soil Quality Guidelines[62] used as limit values in the environmental assessment studies indicates that, except for a few samples with concentrations exceeding the guidelines for agricultural soils (As, Cd, Cr, and Zn), they cannot be considered as being substantially contaminated (Table 1).

The variability plots for trace element concentrations in the soil profiles show that, for the whole dataset, some elements exhibit the highest concentrations in the litter (Cr, Ni), or have a steady concentration profile (Hg, Zn) (Fig. 4). In contrast, the As, Cd, Cu, Pb, Sb and V concentrations increase from the grass to subsoil, followed by a substantial concentration drop in the bedrock (Fig. 4). This is somewhat surprising, given the fact that these contaminants are thought to originate from the smelter- or mine-emissions and should be mainly accumulated in the uppermost soil layers as observed in many mining areas as well as near Tsumeb, but generally closer to the contamination hotspots.[1,8,49] However, the variability in depth-related concentrations is more complex and largely site dependent. Fig. 5 shows that sites downwind of the smelter are slightly more enriched in smelter-derived contaminants, but the concentration data also scatter widely within individual sites. Significantly higher As and Cu concentrations are found in the grass at a site downwind of the smelter, which has not experienced a fire since 2012 (Table S4) and, in comparison with other sites, As (but not other trace elements) is also enriched in the litter at these plots (Fig. 5). This may be related to the accumulation of smelter emissions over 11 years after the fire. Indeed, the Cu smelter currently processes As-rich concentrates and As is considered a serious environmental problem in the area.[3,27,50] On the other hand, the highest As concentrations in the topsoil and subsoil were found at the plots downwind of the smelter burned in 2021 (Fig. 5), which could be related to partial As release from the litter during burning[27] and/or increased leaching after the fire, followed by migration into deeper soil layers, a phenomenon typically observed in (sub)tropical soils exhibiting a low retention capacity for trace elements.[63] Alternatively, the

View Article Online
DOI: 10.1039/D6VA00064A

observed patterns could result from a combination of these two processes. A charcoal layer, forming a topsoil at one plot at this site, exhibits substantially lower contents of As, Cd, Cu, Pb and Zn (Fig. 5), which might be attributed to a smoldering fire regime with higher temperatures leading to losses of these elements.[25] Surprisingly, such a concentration drop has not been observed for Hg (Fig. 5), which is generally assumed to be re-emitted at relatively low temperatures.[19,20] This discrepancy could be attributed to Hg remobilization and subsequent trapping by charred organic matter, as observed in Portuguese shrublands following moderate-severity fires.[64]

The water-leachate concentration data for the litter, topsoil, and subsoil samples are reported in Table S5. A leach test can be used as an indicator of the potential for trace elements to be released into solution after the first contact with rainwater; the adopted fast-leaching test developed by USGS[52] is particularly useful and has been shown to be a good predictor for such estimates in post-fire soils and ashes.[33] Comparisons show that the highest leachabilities were found in the litter samples (Table S5). Whereas many elements were extracted in low concentrations, often below the LODs (Ni, Pb, Cr), substantially higher leachabilities were reported for As (2.6-233 µg/L), Cu (2.6-178 µg/L), and Zn (<DL-519 µg/L) (Table S5; Fig. 6a). For these elements, up to 29%, 25%, and 28% of the total soil concentrations were leached, respectively (Table S5; Fig. 6b). Comparisons with the drinking water guidelines[65] and water quality guidelines for livestock and irrigation[62] revealed that As is a problematic trace element, with values exceeding these regulatory limits, particularly in the litter and topsoil samples (Fig. 6a; Table S5).

The PHREEQC calculations indicated that whereas Cr is leached to a low extent and less toxic Cr^{III} species dominate its redox speciation, the leached As prevails in its oxidized As^{V} form (presumably as arsenates) (Table S5). Moreover, the PHREEQC predictions show that the leachates are highly supersaturated with respect to Fe (oxyhydr)oxides (ferrihydrite,

View Article Online
DOI: 10.1039/D6VA00064A

amorphous $Fe(OH)_3$; goethite, FeOOH) (Table S5). These phases are known to be efficient sorbents of many trace elements.[66] Whereas the sorption efficiency of cationic metals (such as Pb, Cu, or Zn) on Fe (oxyhydr)oxides increases with an increasing pH, and anionic species such as As^V are better retained under acidic conditions.[66-68] Our soil extracts are near-neutral to alkaline (Table S5), leading to significantly higher As leaching from the litter and soil samples. The low Cr and Pb concentrations in our water extracts can be explained by their efficient adsorption by the soil Fe (oxyhydro)oxides under the given conditions (Cr: the pH of 50% adsorption [pH_{50}] is ~4; Pb: pH_{50} is ~4.2). In contrast, the sorption edges of Cu and Zn are shifted to higher pH values[67] and may be leached from the litter and soil samples to a much greater extent.

Nevertheless, the site-specific data (Fig. 6c, d) suggest that the extent of As leaching is not directly dependent on fire effects and is generally more pronounced on sites downwind, which are supposed to receive a higher proportion of smelter emissions, especially in the litter samples. Strong correlations were observed between the water-leachable trace elements (except V) and C_{org}, likely reflecting greater leaching from the litter (Table S6). In contrast, across the entire dataset, water-leachable trace elements did not correlate with soil pH and, for most of them, with their total elemental content (Table S6).

To gain a deeper understanding of post-fire changes in the trace-element geochemistry, we compared unburned and burned plots from a 2023 fire event. The data (Table S4) and their visualization in heatmaps (Fig. 7) show that, especially the litter, which is considered the most affected by fires[34], exhibits changes in the total concentrations when burned. The ash (burned litter) shows higher concentrations of Cd, Cr, Cu, Ni, Pb, V, and Zn, with less pronounced increases in As, Co, and Sb (Figs 7a and 5; Table S4). Only for Zn, the differences were statistically significant (Fig. 7a). Similarly, the highest differences between the unburned and burned soils (and the pre- and postfire watershed waters) were found for Zn

View Article Online
DOI: 10.1039/D6VA00064A

from the wildland-urban interfaces after large fires in the United States.[11,34] However, in these areas, the increases in concentrations of Zn and other metallic elements were mainly attributed to burned anthropogenic materials (building structures, vehicles, pipes, wires, or paint)[11,33,34], which cannot be the case with our samples. In contrast, an increase in concentration after fire was not observed for Hg, which appears to be released back into the atmosphere, even at low-temperature fires.[20] The differences between the unburned and burned topsoils and subsoils were not so pronounced except for Cd, Cu, Pb, and Zn (Table S4; Figs 7a and 5).

Depletion or enrichment relative to the background is reflected in the EFs calculated for the individual trace elements (Table S7). It was found that, with respect to the bedrock, the grass was especially enriched in all the trace elements except V (EF ranging from 6.5 to 356), whereas the enrichment of the litter was not so pronounced (EF ranging from 1.2 to 44.9) (Table S7; Fig. 7b). When the burned and unburned samples are compared, an increase in the EFs corresponds to the enrichment of a given element during the fire and a decrease in the EFs means re-emission (or loss) of a given element. A comparison of the mean values of EFs between the unburned and burned litter (calculated from three sampled plots) indicates that, whereas some elements do not exhibit any changes (Cr, Ni), others are lost (e.g., Hg by a factor of ~2) (Table S7). Copper, Pb, and Zn are especially enriched in the ash (by a factor of ~2), but the difference was statistically significant only for Zn (ANOVA, Tukey's test, $P < 0.05$) (Table S7; Fig. 7b). Arsenic is also enriched, but significantly less than other main pollutants, suggesting its partial re-emission during fire (Table S7; Fig. 7b).

Based on the literature[23,35,69], we expected that trace element leaching would be significantly higher in the burned plots than in the unburned plots. Surprisingly, our data show contrasting results for the litter: leaching of Cu and Zn significantly decreased (ANOVA, Tukey's test; $P < 0.0243$ and $P < 0.0001$, respectively), whereas leaching of other elements did not differ

View Article Online
DOI: 10.1039/D6VA00064A

significantly. On the other hand, postfire increases in the leaching of As, Cu, and Zn were observed for the topsoils, but the differences between the unburned and burned plots were not statistically significant (Fig. S7).

Source tracing using lead isotopes

The Pb isotopic compositions of the studied samples, as well as the potential local and regional Pb sources, are plotted in a 3-isotope graph ($^{206}Pb/^{207}Pb$ versus $^{208}Pb/^{206}Pb$; Fig. 8a) and as a boxplot diagram (Fig. 8b). The whole dataset is given in Table S8. Whereas most of the soil data cluster around the $^{206}Pb/^{207}Pb$ ratio of 1.164 (range: 1.138–1.185), the $^{206}Pb/^{207}Pb$ isotopic signatures of the grass are lower (median: 1.138, range 1.121–1.155) and those of the bedrock are substantially higher (median: 1.185, range 1.182–1.210) (Table S6; Fig. 8). The $^{206}Pb/^{207}Pb$ values of the grass statistically differ from the other sample categories (ANOVA, Tukey's test, $P < 0.0001$) (Fig. 8b). The difference in Pb isotopic compositions between the samples from the unburned and burned plots of the 2023 fire event remain within the standard deviation of the measurement and/or intra-site variability and are not statistically significant.

However, the Pb isotopic compositions of the studied samples can be compared with the potential Pb sources (Fig. 8a). Unfortunately, the Pb isotopic signatures of the local ore (Kamona et al.[38]) overlap with that of gasoline ($^{206}Pb/^{207}Pb$ of 1.150; Mihaljevič et al.[46]) and the influence of legacy leaded petrol can hardly be recognized in the study area. Thus, it cannot be concluded, as in other recent Pb isotopic studies, that most of the Pb found in the ash originates from past petrol-derived Pb deposition[29,53] or that petrol-derived Pb can be remobilized back to the atmosphere.[26,28] The Pb originating from slag heaps and mine tailings disposal sites roughly correspond to the signature of the Tsumeb ores, with several samples

View Article Online
DOI: 10.1039/D6VA00064A

showing slightly lower $^{206}Pb/^{207}Pb$ values, which can reflect processing of ore of other origin (median $^{206}Pb/^{207}Pb$: 1.153, range: 1.132–1.157). These values closely correspond to dusts recently analyzed by Fry et al.[70] around the Tsumeb agglomeration (median: 1.150, range: 1.130–1.170), showing that the legacy of mining and smelting activities still prevails in the studied area, at least near the contamination hotspots. Whereas the studied soils exhibit a Pb isotopic composition ranging between the signatures of the local ore mining and natural background (bedrock), the grass samples follow a binary mixing model between south-African aerosols (median $^{206}Pb/^{207}Pb$: 1.076)[71] and the signature of local mining and ore processing (median $^{206}Pb/^{207}Pb$: 1.155), with the prevailing contribution of the latter (57-99%; Fig. 8). The dust from nearby desert areas (Namib desert situated W and SW of Tsumeb), influencing the composition of the atmospheric aerosols mostly downwind, i.e., above the southern Atlantic Ocean[72], can be excluded from the local sources because of their highly radiogenic signature ($^{206}Pb/^{207}Pb > 1.20$). Similarly, the Pb isotopic signatures of flue dusts from the currently operating Cu smelter in Tsumeb exhibit $^{206}Pb/^{207}Pb$ values of 1.189–1.193, which do not correspond to the Pb isotopic compositions of the litter and surface soils.

General discussion and environmental implications

We observed a high spatial variability in the trace element concentrations at the vegetation-litter-topsoil-subsoil interface (Table 1; Figs 4 and 5). The study sites are not directly adjacent to the smelter and former mining area (distance to the primary pollution source varies from ~9 to 20 km), which is the reason for the not excessively elevated trace element concentrations in the studied samples (Table 1). Nevertheless, depth-related concentration patterns (Fig. 3) indicate that As, Cd, Cu, Hg, Pb, Sb, and Zn are significantly above background levels and are likely associated with airborne contamination. The Pb isotopic tracing indicates that legacy Pb from the historical mining and smelting of the local ore still

View Article Online
DOI: 10.1039/D6VA00064A

predominates in the soils, even though Pb smelting in Tsumeb ceased in the 1990s and the Pb smelter was finally dismantled in the 2010s. In contrast, the Pb isotopic signal of the currently operating Cu smelter does not correspond to the isotopic compositions of the Pb found in the studied samples (Fig. 6). It can nevertheless be expected that, despite the existing flue gas cleaning technologies, the smelter remains the source of the metal(loid)-bearing emissions. Previous studies found that the As-rich dust composed mainly of highly soluble arsenolite (As_2O_3) and adhering to the surfaces of vegetation in the vicinity of the Tsumeb smelter[3,25] can dissolve when deposited in the soils, leading to downward As migration.[73] The elevated As (but not Pb) concentrations in the litter at the plots burned in 2012 (Table S4) may thus be related to an ongoing long-term accumulation of smelter emissions transported on a regional scale downwind of the smelter stack. Another explanation for the higher As concentrations in the litter at the given plots, compared to Pb, could be related to the difference in the chemical composition of the aerosols emitted by the smelter. Csavina et al.[74] studied aerosols emitted from the Hayden Cu smelter (Arizona, USA) and found different proportions of As and Pb in various size fractions. Whereas smaller aerosols, which could travel longer distances and contained more As, Pb dominated in the coarser ones.[74]

Fire impacts on the trace element concentrations in soils are variable and depend on multiple factors. We acknowledge the complexity of these processes, which include the role of the vegetation and soil chemistry, moisture content, and solid-phase speciation of trace elements in the burned material, intensity and duration of the fire, and others.[11,20,22,25,27,56,75] Compared to experimental studies conducted on vegetation or soils with high trace element concentrations and known speciation[20,25] or postfire investigations in urban areas[11], former mining areas[12-14,17] and natural geochemical anomalies[30,31], our results are not so straightforward. Due to high within- and between-site variability and the scattering of the concentration data (Figs 4 and 5), some interpretations remain speculative and not

View Article Online
DOI: 10.1039/D6VA00064A

statistically significant. For instance, the ash from the 2023 fire event exhibits higher concentrations of smelter-derived elements (As, Cd, Cu, Pb, Sb, Zn) as well as an increase in the EFs of some elements in comparison with the unburned litter. Still, the changes are statistically significant only for Zn (Fig. 7).

The dark brown to black ash at the site burned in 2023 (Fig. S5) indicates a lower-intensity fire with temperatures probably <400 °C.[60,61] Moreover, fast-moving fires can be expected in these savanna environments, accompanied by a short and shallow heating of the soil surface.[36] There are other reasons for supporting these temperature estimates:

(i) Although not statistically significant, a drop in the Hg concentration and EF_{Hg} in the burned litter (Figs 5 and 7; Tables S4 and S6) agrees well with the field data from other sites showing Hg re-emission.[16,18] The experimental studies confirmed that a significant portion of Hg is released back to the atmosphere at relatively low temperatures, around 340 °C.[20]

(ii) The As enrichment in the ash is not so pronounced compared to other smelter-derived contaminants (Table S4), and no significant change in EF_{As} was observed (Table S6). The partial emission of As might occur because experimental studies show that, at temperatures <400 °C, As is remobilized back to the atmosphere when bound in organic species or arsenolite, as documented in vegetation and soils in the Tsumeb area.[25,27] In contrast, such remobilization cannot be assumed for other trace elements (Cd, Cu, Pb, Zn), which exhibit re-emissions at much higher temperatures (>550-600 °C).[25]

(iii) Johnston et al.[76] simulated fire effects on As-rich soils by heating mixtures of soils and As^{V}-bearing ferrihydrite [$Fe(OH)_3$] and goethite (FeOOH) in the temperature range 200–800 °C. They found that at temperatures above 400 °C, these minerals transform to maghemite (Fe_2O_3), and arsenic is rapidly reduced to As^{III}, becoming more mobile.[76] We have evidence that this redox transformation has not occurred because the PHREEQC speciation

View Article Online
DOI: 10.1039/D6VA00064A

calculations confirm that all the As leached from the litter is pentavalent, suggesting that the fire temperatures at our studied plots were likely below 400 °C.

(iv) Similarly, fires were found to be responsible for the Cr oxidation to a more toxic Cr^{VI} species.[30,31] A recent study investigating the effects of the landscape position and related burn intensity on the Cr redox transformation in the surface soil found that the maximum Cr^{VI} was generated in summit soils burned at 400 °C, and its concentration decreased downslope, where lower burning temperatures were expected.[31] Moreover, the authors found that the oxidized Cr (forming oxyanionic species) was easily leached out of these post-fire soils.[31] These findings are in clear contrast with the results of our leaching tests coupled to the PHREEQC modeling, where we found that very low Cr amounts are extracted from the litter and soil, and the speciation is dominated by Cr^{III} species (Table S5), which confirms again that temperatures likely did not likely exceed 400 °C.

The overall concentration increases from the litter to the subsoil, as observed for many trace elements, appears to be related to downward leaching (as indicated by water extracts, especially for As, Cu, and Zn) (Fig. 6; Table S5). Such mobilization can be enhanced by fires, leading to increased soil pH in burned areas. We hypothesize that even moderately contaminated areas in semiarid savanna environments, which experience frequent fires during the dry season, can become sources of contaminants when re-wetted by the first heavy rains of the wet season (October/November in Namibia). More research in such semiarid areas of sub-Saharan Africa is needed to better understand these phenomena and the environmental risks for the quality of local water resources and land used by farmers and local communities.

Conclusions

View Article Online
DOI: 10.1039/D6VA00064A

This study demonstrates the variability in the spatial distributions of trace elements at the vegetation-litter-soil interface along a chronosequence, ranging from freshly burned areas to 11-year post-fire sites, situated near a non-ferrous smelter in the northern Namibian savanna. Using Pb isotopic tracing, we found that legacy mining and smelting activities are responsible for the Pb dispersion in the area. However, the ongoing processing of As-rich Cu concentrates at the currently operating Cu smelter is likely responsible for the elevated As concentrations in the litter accumulated after the 2012 fire event and collected downwind of the smelter. When the unburned and burned plots were compared, the changes in trace element concentrations were most significant in the litter and topsoils. The within-site and between-site variability in the trace elements concentration patterns reflects the combined effects of site position with respect to the smelter stack, fire regimes and potential downward leaching. Multiple observations (ash color, changes in total concentrations, enrichment factors) suggest that the fires in the area were of low intensity with temperatures <400 °C, leading to partial re-emission of Hg and, to a lesser extent, also As. Other smelter-derived contaminants are concentrated in the ash, except one plot burned in 2021, where a charcoal layer indicated much higher temperatures corresponding to a smoldering fire. Wildland fires in the studied area resulted in a loss of organic carbon and an increase in soil pH, which, in turn, may enhance As leaching. Arsenic remains the most problematic contaminant, as its short-term mobilization might threaten local water resources, especially in the early wet season.

Electronic Supplementary Information

Electronic Supplementary Information (ESI) contains (1) one text file with 7 figures and 7 tables and (2) one Excel file with 4 large tables.

View Article Online
DOI: 10.1039/D6VA00064A

Data availability

The data for this article are included as part of the Supplementary Information and are also available at Zenodo at https://doi.org/10.5281/zenodo.18497577.

Authors' contributions

Vojtěch Ettler: Conceptualization, Data curation, Formal analysis, Funding acquisition, Investigation, Methodology, Project Administration, Resources, Supervision, Validation, Visualization, Roles/Writing - original draft, Writing - review & editing

Martin Mihaljevič: Data curation, Formal analysis, Funding acquisition, Investigation, Project administration, Resources, Writing - review & editing

Tereza Zádorová: Data curation, Formal analysis, Investigation, Resources, Writing - review & editing

Daniel Žížala: Investigation, Resources, Writing - review & editing

Bohdan Kříbek: Data curation, Investigation, Project administration, Resources, Writing - review & editing

Aleš Vaněk: Investigation, Resources, Writing - review & editing

Vít Penížek: Investigation, Resources

Ondra Sracek: Investigation, Resources, Writing - review & editing

Ban Mapani: Investigation, Project administration, Resources, Writing - review & editing

Conflict of interest

View Article Online
DOI: 10.1039/D6VA00064A

The authors declare that they have no known competing financial interests or personal relationships that could have appeared to influence the work reported in this paper.

Acknowledgements

This study was supported by the Czech Science Foundation (GAČR project 23-05051S) and the Johannes Amos Comenius Programme (P JAC), project No. CZ.02.01.01/00/22_008/0004605, Natural and anthropogenic georisks. We thank many colleagues for their help in the laboratory (Marie Fayadová, Věra Vonásková, Lenka Jílková). Alan Harvey Cook is also thanked for revising the English in this manuscript. We are grateful to Prof. Kevin C. Jones for editorial handling of the manuscript and two anonymous reviewers whose pertinent comments helped to substantially improve the original version of the manuscript.

References

(1) V. Ettler, Soil contamination near non-ferrous metal smelters: A review, *Appl. Geochem.,* 2016, **64**, 56–74, https://doi.org/10.1016/j.apgeochem.2015.09.020

(2) B. Mapani, R. Ellmies, L. Hahn, G. Schneider, K. Ndalulilwa, R. Leonard, M. Zeeuw, N. Mwananawa, S. Uugulu, E. Namene, W. Amaambo, F. Sibanda, M. Mufenda, Contamination of agricultural products in the surrounding of the Tsumeb smelter complex, *Comm. Geol. Surv. Namibia*, 2014, **15**, 92–110.

(3) B. Kříbek, V. Majer, I. Knésl, J. Keder, B. Mapani, F. Kamona, M. Mihaljevič, V. Ettler, V. Penížek, A. Vaněk, O. Sracek, Contamination of soil and grass in the Tsumeb smelter area, Namibia: Modeling of contaminants dispersion and ground geochemical verification, *Appl. Geochem*., 2016, **64**, 75–91, https://doi.org/10.1016/j.apgeochem.2015.07.006

(4) J. Csavina, J. Field, M.P. Taylor, S. Gao, A. Landázuri, E.A. Betterton, A.E. Sáez, A review on the importance of metals and metalloids in atmospheric dust and aerosol from mining operations. *Sci. Total Environ.*, 2012, **433**, 58–73, https://doi.org/10.1016/j.scitotenv.2012.06.013

(5) J. Kasongo, L.Y. Alleman, J.M. Kanda, A. Kaniki, V. Riffault, Metal-bearing airborne particles from mining activities: A review on their characteristics, impacts and research perspectives. *Sci. Total Environ.*, 2024, **951**, 175426, https://doi.org/10.1016/j.scitotenv.2024.175426

(6) X. Hou, M. Parent, M.M. Savard, N. Tassé, C. Bégin, J. Marion, Lead concentrations and isotope ratios in the exchangeable fraction: tracing soil contamination near a copper smelter, *Geochem. Explor. Environ. Anal.*, 2006, **6**, 229–236, https://doi.org/10.1144/1467-7873/05-092

(7) C.M. Zdanowicz, C.M. Banic, D.A. Pactunc, D.A. Kliza-Petelle, Metal emissions from a Cu smelter, Rouyn-Noranda, Québec: characterization of particles sampled in air and snow. *Geochem. Explor. Environ. Anal.*, 2006, **6**, 147–162, https://doi.org/10.1144/1467-7873/05-089

(8) V. Ettler, L. Konečný, L. Kovářová, M. Mihaljevič, O. Šebek, B. Kříbek, V. Majer, F. Veselovský, V. Penížek, A. Vaněk, I. Nyambe, Surprisingly contrasting metal distribution and fractionation patterns in copper smelter-affected tropical soil in forested and grassland areas (Mufulira, Zambian Copperbelt), *Sci. Total Environ.*, 2014, **473–474**, 117–124, https://doi.org/10.1016/j.scitotenv.2013.11.146

(9) A.L.R. Westerling, Increasing western US forest wildfire activity: sensitivity to changes in the timing of spring, *Phil. Trans. R. Soc. B*, 2016, **371**, 20150178, https://doi.org/10.1098/rstb.2015.0178

View Article Online
DOI: 10.1039/D6VA00064A

(10) M. Goss, D.L. Swain, J.T. Abatzoglou, A. Sarhadi, C.A. Kolden, A.P. Williams, N.S. Diffenbaugh, Climate change is increasing the likelihood of extreme autumn wildfire conditions across California, *Environ. Res. Lett.*, 2020, **15**, 094016. https://doi.org/10.1088/1748-9326/ab83a7

(11) S. Jech, C. Adamchak, S.C. Stokes, M.E. Wiltse, J. Callen, J. VanderRoest, E.F. Kelly, E.L.S. Hinckley, H.J. Stein, T. Borch, N. Fierer, Determination of soil contamination at the wildland-urban interface after the 2021 Marshall Fire in Colorado, USA, *Environ. Sci. Technol.*, 2024, **58**, 4326–4333, https://doi.org/10.1021/acs.est.3c08508

(12) J. Abraham, K. Dowling, S. Florentine, Controlled burn and immediate mobilization of potentially toxic elements in soil, from a legacy mine site in Central Victoria, Australia, *Sci. Total Environ*, 2018, **616–617**, 1022–1034, https://doi.org/10.1016/j.scitotenv.2017.10.216

(13) J. Abraham, K. Dowling, S. Florentine, Influence of controlled burning on the mobility and temporal variations of potentially toxic metals (PTMs) in the soils of a legacy gold mine site in Central Victoria, Australia, *Geoderma*, 2018, **331**, 1–14, https://doi.org/10.1016/j.geoderma.2018.06.010

(14) C.S. Tshisikhawe, V.M. Ngole-Jeme, Temperature induced changes on heavy metal geochemical partitioning and mobility in contaminated and uncontaminated soils. *Environ. Pollut. Bioavail.*, 2024, **36**, 2317747, https://doi.org/10.1080/26395940.2024.2317747

(15) M. Mihaljevič, V. Ettler, O. Šebek, O. Sracek, B. Kříbek, T. Kyncl, V. Majer, F. Veselovský, Lead isotopic and metallic pollution record in tree rings from the Copperbelt Mining-Smelting Area, Zambia, *Water Air Soil Pollut.*, 2011, **216**, 657–668, https://doi.org/10.1007/s11270-010-0560-4

(16) I. Campos, C. Vale, N. Abrantes, J.J. Kaizer, P. Pereira, Effects of wildfire on mercury mobilization in eucalypt and pine forests, *Catena*, 2015, **131**, 149–159, https://doi.org/10.1016/j.catena.2015.02.024

(17) J. Abraham, K. Dowling, S. Florentine, Effects of prescribed fire and post-fire rainfall on mercury mobilization and subsequent contamination assessment in a legacy mine site in Victoria, Australia, *Chemosphere*, 2018, **190**, 144–153, https://doi.org/10.1016/j.chemosphere.2017.09.117

(18) A.M.D. Vieira, M. Vaňková, I. Campos, J. Trubač, R. Baieta, M. Mihaljevič, Estimation of mercury emissions from the forest floor of a pine plantation during a wildfire in central Portugal, *Environ. Monit. Assess.*, 2022, **194**, 755, https://doi.org/10.1007/s10661-022-10436-7

(19) R.K. Kolka, K.M. Quigley, J.R. Miesel, M.B. Dickinson, B.R. Sturtevant, C.C. Kern, Influence of barrens restoration treatments on soil carbon, nitrogen, and mercury pools and emissions, *Soil Sci. Soc. Am. J.*, 2023, **88**, 584–592, https://doi.org/10.1002/saj2.20657

(20) M. Tuhý, J. Rohovec, Š. Matoušková, M. Mihaljevič, B. Kříbek, A. Vaněk, B. Mapani, H. Göttlicher, R. Steininger, J. Majzlan, V. Ettler, The potential wildfire effects on mercury remobilization from topsoils and biomass in a smelter-polluted semiarid area, *Chemosphere*, 2020, **247**, 125972, https://doi.org/10.1016/j.chemosphere.2020.125972

(21) R. Terzano, I. Rascio, I. Allegretta, C. Porfido, M. Spagnuolo, M.Y. Khanghani, C. Crecchio, F. Sakellariadou, C.E. Gattullo, Fire effects on the distribution and bioavailability of potentially toxic elements (PTEs) in agricultural soils, *Chemosphere*, 2021, **281**, 130752, https://doi.org/10.1016/j.chemosphere.2021.130752

(22) M.L. Fernandez-Marcos, Potentially toxic substances and associated risks in soils affected by wildfires: A review, *Toxics*, 2022, **10**, 31, https://doi.org/10.3390/toxics10010031

(23) I. Campos, N. Abrantes, J.J. Kaizer, C. Vale, P. Pereira, Major and trace elements in soils and ashes of eucalypt and pine forest plantations in Portugal following a wildfire, *Sci. Total. Environ*., 2016, **572**, 1363–1376, https://doi.org/10.1016/j.scitotenv.2016.01.190

(24) C. Santín, S.H. Doerr, X.L. Otero, C.J. Chafer, Quantity, composition and water contamination potential of ash produced under different wildfire severities. *Environ. Res*., 2015, **142**, 297–308, https://doi.org/10.1016/j.envres.2015.06.041

(25) M. Tuhý, V. Ettler, J. Rohovec, Š. Matoušková, M. Mihaljevič, B. Kříbek, B. Mapani, Metal(loid)s remobilization and mineralogical transformations in smelter-polluted savanna soils under simulated wildfire conditions, *J. Environ. Monit.*, 2021, **293**, 112899, https://doi.org/10.1016/j.jenvman.2021.112899

(26) R. Baieta, A.M.D. Vieira, M. Vaňková, M. Mihaljevič, Effects of forest fires on soil lead elemental contents and isotopic ratios, *Geoderma*, 2022, **414**, 115760, https://doi.org/10.1016/j.geoderma.2022.115760

(27) M. Tuhý, V. Ettler, J. Rohovec, K. Stonová, Š. Matoušková, P. Drahota, A.L.Sullivan, Thermally-induced release of arsenic from minerals and phases relevant to polluted natural systems affected by wildfires, *Appl. Geochem.*, 2025, **182**, 106318, https://doi.org/10.1016/j.apgeochem.2025.106318

(28) C.F. Isley, M.P. Taylor, Atmospheric remobilization of natural and anthropogenic contaminants during wildfires, *Environ. Pollut.*, 2020, **267**, 115400, https://doi.org/10.1016/j.envpol.2020.115400

View Article Online
DOI: 10.1039/D6VA00064A

(29) K.O. Odigie, A.R. Flegal, Trace metal inventories and lead isotopic composition chronicle a forest fire's remobilization of industrial contaminants deposited in the Angeles National Forest, *PLoS One*, 2014, **9**, e107835, https://doi.org/10.1371/journal.pone.0107835

(30) A.M. Lopez, J.L. Pacheco, S. Fendorf, Metal toxin threat in wildland fires determined by geology and fire severity, *Nat. Commun.*, 2023, **14**, 8007, https://doi.org/10.1038/s41467-023-43101-9

(31) C.S. Obeidy, M.W. Koeneke, O.W. Duckworth, M. L. Polizzotto, Landscape position and burn intensity influence heat-induced soil chromium contamination, *Environ. Sci. Technol.*, 2025, **59**, 25842–25852, https://doi.org/10.1012/acs.est.5c08315

(32) J.M. Cerrato, J.M. Blake, C. Hirani, A.L. Clark, A.M.S. Ali, K. Artyushova, E. Peterson, R.L. Bixby, Wildfires and water chemistry: effects of metals associated with wood ash, *Environ. Sci.: Process. Impacts*, 2016, **18**, 1078–1089. https://doi.org/10.1039/c6em00123h

(33) C.A. Burton, T.M. Hoefen, G.S. Plumlee, K.L. Baumberger, A.R. Backlin, E. Gallegos, R.N. Fisher, Trace elements in stormflow, ash, and burned soil following the 2009 Station Fire in southern California, *PLoS One*, 2016, **11**, e0153372, https://doi.org/10.1371/journal.pone.0153372

(34) L.J. Magliozzi, S.J. Matiasek, C.N. Alpers, J.A. Korak, D. McKnight, A.L. Foster, J.N. Ryan, D.A. Roth, P. Ku, M.T.K. Tsui, A.T. Chow, J.P. Webster, Wildland-urban interface wildfire increases metal contributions to stormwater runoff in Paradise, California. *Environ. Sci.: Process. Impacts*, 2024, **26**, 667–685, https://doi.org/10.1039/d3em00298e

(35) M.J. Gunnarsdottir, S. Tómasdóttir, O. Őrlygsson, H.Ó. Andradóttir, S.M. Gardarsson, Impact of wildfires on the drinking water catchment for the capital area of Iceland – a case study. *Environ. Sci.: Adv.*, 2025, **4**, 606–618. https://doi.org/10.1039/d4va00352g

(36) S.H. Doerr, A. Girona-García, C. Sánchez-García, D. Badía-Villas, R. Bryant, M.B. Dickinson, R. Hsieh, J. Mataix-Solera, J.R. Miesel, P.R. Robichaud, C.R. Stoof, C. Santín, Soil heating during wildfires and prescribed burns: a global evaluation, *Int. J. Wildland Fire*, 2025, **34**, WF25103, https://doi.org/10.1071/WF25103

(37) G. Schneider, *The wonders of the Otavi Mountainland: Minerals, fossils and underground lake*s. In: Anhauesser, C.R., Viljoen, M.J., & Viljoen, R.P. (Eds) Africa's Top Geological Sites. Struik Nature, Cape Town, 2016, pp. 151–155.

(38) A.F. Kamona, J. Lévêque, G. Friedrich, U. Haack, Lead isotopes of the carbonate-hosted Kabwe, Tsumeb, and Kipushi Pb-Zn-Cu sulphide deposits in relation to Pan African orogenesis in the Damaran-Lufilian Fold Belt of Central Africa, *Miner. Depos.*, 1999, **34**, 273–283, https://doi.org/10.1007/s001260050203

(39) V. Ettler, Z. Johan, B. Kříbek, O. Šebek, M. Mihaljevič, Mineralogy and environmental stability of slags from the Tsumeb smelter, Namibia, *Appl. Geochem.*, 2009, **24**, 1–15, https://doi.org/10.1016/j.apgeochem.2008.10.003

(40) A. Jarošíková, V. Ettler, M. Mihaljevič, B. Kříbek, B. Mapani, The pH-dependent leaching behavior of slags from various stages of a copper smelting process: Environmental implications, *J. Environ. Manage.*, 2017, **187**, 178–186, https://doi.org/10.1016/j.envman.2016.11.037

(41) O. Sracek, V. Ettler, M. Mihaljevič, B. Kříbek, B. Mapani, V. Penížek, T. Zádorová, A. Vaněk, Identification of processes in Cu-ore heap leaching using Cu isotopes and

leachate chemistry at Tschudi mine, northern Namibia, *Hydrometallurgy*, 2024, **228**, 106356, https://doi.org/10.1016/j.hydromet.2024.106356

(42) V. Ettler, Z. Johan, B. Kříbek, F. Veselovský, M. Mihaljevič, A. Vaněk, V. Penížek, V. Majer, O. Sracek, B. Mapani, F. Kamona, I. Nyambe, Composition and fate of mine- and smelter-derived particles in soils of humid subtropical and hot semiarid areas, *Sci. Total Environ.*, 2016, **563–564**, 329–339, https://doi.org/10.1016/j.scitotenv.2016.04.133

(43) B. Kříbek, A. Šípková, V. Ettler, M. Mihaljevič, V. Majer, I. Knésl, B. Mapani, V. Penížek, A. Vaněk, O. Sracek, Variability of the copper isotopic composition in soil and grass affected by mining and smelting in Tsumeb, Namibia, *Chem. Geol.*, 2018, **493**, 121–135, https://doi.org/10.1016/j.chemgeo.2018.05.035

(44) IUSS Working Group WRB, *World Reference Base for Soil Resources. International soil classification system for naming soils and creating legends for soil maps*, 4th edition, IUSS, Vienna, 2022.

(45) Atlas of Namibia Team, *Atlas of Namibia: its land, water and life*, Namibia Nature Foundation, Windhoek, 2022.

(46) M. Mihaljevič, V. Ettler, A. Vaněk, V. Penížek, M. Svoboda, B. Kříbek, O. Sracek, B.S. Mapani, A.F. Kamona, Trace elements and the lead isotopic record in marula (*Sclerocarya birrea*) tree rings and soils near the Tsumeb smelter, Namibia, *Water Air Soil Pollut.*, 2015, **226**, 177, https://doi.org/10.1007/s11270-015-2440-4

(47) T. Zádorová, V. Penížek, M. Mihaljevič, M. Koubová, L. Lisá, V. Ettler, V. Tejnecký, O. Drábek, L. Pavlů, B. Kříbek, A. Vaněk, O. Sracek, J.R. Royas, T. Hrdlička, P. Vokurková, B. Mapani, Local diversity of soil forming processes in the semi-arid tropics and its environmental drivers: An example from Otavi Mountains, northern Namibia, *Catena*, 2025, **249**, 108671, https://doi.org/10.1016/j.catena.2024.108671

(48) GEMAS, *EuroGeoSurveys Geochemical mapping of agricultural and grazing land soil of Europe (GEMAS) - Field manual*. Report 2008.038. Geological Survey of Norway, Trondheim, 2008, 46 p.

(49) F. Podolský, V. Ettler, O. Šebek, J. Ježek, M. Mihaljevič, B. Kříbek, O. Sracek, A. Vaněk, V. Penížek, V. Majer, B. Mapani, F. Kamona, I. Nyambe, Mercury in soil profiles from metal mining and smelting areas in Namibia and Zambia: distribution and potential sources, *J. Soils Sedim.*, 2015, **15**, 648–658. https://doi.org/10.1007/s11368-014-1035-9

(50) A. Jarošíková, V. Ettler, M. Mihaljevič, P. Drahota, A. Culka, M. Racek, Characterization and pH-dependent environmental stability of arsenic trioxide-containing copper smelter flue dust, *J. Environ. Manage.*, 2018a, **209**, 71–80, https://doi.org/10.1016/j.envman.2017.12.044

(51) ISO 10390, *Soil, treated biowaste and sludge – Determination of pH*, ISO, Geneva, 2021.

(52) P.L. Hageman, *U.S. Geological Survey field leach test for assessing water reactivity and leaching potential of mine waste, soils, and other geological and environmental materials*, U.S. Geological Survey Techniques and Methods, book 5, chapter D3, 14, 2007, https://pubs.usgs.gov/tm/2007/05D03/

(53) K.O. Odigie, A.R. Flegal, Pyrogenic remobilization of historic industrial lead depositions, *Environ. Sci. Technol.*, 2011, **45**, 6290–6295, https://doi.org/10.1021/es200944w

(54) M. Strzelec, B.C. Proemse, L.A. Barmuta, M. Gault-Ringold, M. Desservettaz, P.W. Boyd, M.M.G. Perron, R. Schofield, A.R. Bowie, Atmospheric trace metal deposition

from natural and anthropogenic sources in western Australia, *Atmosphere*, 2020, **11**, 474; https://doi.org/10.3390/atmos11050474

(55) D.L. Parkhurst, C.A.J. Appelo, *Description of input and examples for PHREEQC version 3–A computer program for speciation, batch-reaction, one-dimensional transport, and inverse geochemical calculations*, U.S. Geological Survey Techniques and Methods, book 6, chap. A43, 2013.

(56) D. Badía, S. López-García, C. Martí, O. Ortíz-Perpiñá, A. Girona-García, J. Casaova-Gascón, Burn effects on soil properties associated to heat transfer under contrasting moisture content, *Sci. Total Environ.*, 2017, **601–602**, 1119–1128, https://doi.org/10.1016/j.scitotenv.2017.05.254

(57) M.A. Santoso, X. Huang, N. Prat-Guitart, E. Christensen, Y. Hu, G. Rein, Smoudering fires and soils, in *Fire Effects on Soil Properties*, ed. P. Pereira, J. Mataix-Solera, X. Úbeda, G. Rein, A. Cerdà, CSIRO Publishing, Clayton South, 2019, chapter 13, 203–216.

(58) C. Santín, S. Doerr, Carbon, in *Fire Effects on Soil Properties*, ed. P. Pereira, J. Mataix-Solera, X. Úbeda, G. Rein, A. Cerdà, CSIRO Publishing, Clayton South, 2019, chapter 7, 115–128.

(59) E.U. Hobley, A.J. Le Gay Brereton, B. Wilson, Forest burning affects quality and quantity of soil organic matter, *Sci. Total Environ.*, 2017, **575**, 41–49, https://doi.org/10.1016/j.scitotenv.2016.09.231

(60) A. Bento-Gonçalves, A. Vieira, X. Úbeda, D. Martin, Fire and soils: Key concepts and recent advances, *Geoderma*, 2012, **191**, 3–13, https://doi.org/10.1016/j.geoderma.2012.01.004

DOI: 10.1039/D6VA00064A

(61) M.B. Bodí, D.A. Martin, V.N. Balfour, C. Santín, S.H. Doerr, P. Pereira, A. Cerdà, J. Mataix-Solera, Wildland fire ash: Production, composition and eco-hydrogeomorphic effects. *Earth Sci. Rev.*, 2014, **130**, 103–127, https://doi.org/10.1016/jearscirev.2013.12.007

(62) Canadian Council of Ministers of the Environment (CCME), *Canadian Environmental Quality Guidelines*, 2025, https://ccme.ca/en/current-activities/canadian-environmental-quality-guidelines (Accessed December 2, 2025)

(63) J. Rieuwerts, The mobility and bioavailability of trace metals in tropical soils: a review, *Chem. Spec. Bioavail.*, 2007, **19**, 75–85, https://doi.org/10.3184/095422907X211918

(64) M. Méndez-López, C.T. Jiménez-Morillo, F. Fonseca, T. de Figueiredo, A. Parente-Sendín, F. Alonso-Vega, M. Arias-Estévez, J.C. Nóvoa-Muñoz, Mercury mobilization in shrubland after a prescribed fire in NE Portugal: Insight on soil organic matter composition and different aggregate size, *Sci. Total. Environ.*, 2023, **904**, 167532, https://doi.org/10.1016/j.scitotenv.2023.167532

(65) WHO, Guidelines for drinking water quality, 4th editions, World Health Organization, Geneva, Switzerland, 2022. https://www.who.int/publications/i/item/9789240045064

(66) M. Komárek, A. Vaněk, V. Ettler, Chemical stabilization of metals and arsenic in contaminated soils using oxides – A review, *Environ. Pollut.*, 2013, **172**, 9–22, https://doi.org/10.1016/j.envpol.2012.07.045

(67) C.A.J. Appelo, D. Postma, *Geochemistry, groundwater and pollution*, 2nd Ed., A.A. Balkema Publishers, Leiden, 2005.

(68) Y. Masue, R.H. Loeppert, T.A. Kramer, Arsenate and arsenite adsorption and desorption behavior on coprecipitated aluminium:iron hydroxides, *Environ. Sci. Technol.*, 2007, **41**, 837–842, https://doi.org/10.1021/es061160z

(69) M.P. Burke, T.S. Hogue, A.M. Kinoshita, J. Barco, C. Wessel, E.D. Stein, Pre- and post-fire pollutant loads in an urban fringe watershed in Southern California, *Environ. Monit. Assess.*, 2013, **185**, 10131–10145, https://doi.org/10.1007/s10661-013-3318-9

(70) K.L. Fry, C.A. Wheeler, M.M. Gillings, A.R. Flegal, M.P. Taylor, Anthropogenic contamination of residential environments from smelter As, Cu and Pb emissions: Implications for human health, *Environ. Pollut.*, 2020, **262**, 114235, https://doi.org/10.1016/j.envpol.2020.114235

(71) A. Bollhöfer, K.J.R. Rosman, Isotopic source signatures for atmospheric lead: The Southern Hemisphere, *Geochim. Cosmochim. Acta*, 2000, **64**, 3251–3262, https://doi.org/10.1016/S0016-7037(00)00436-1

(72) S. Gili, A. Vanderstraeten, A. Chaput, J. King, S.M., Gaiero, B. Delmonte, P. Vallelonga, P. Formenti, C. Di Biagio, M. Cazanau, E. Pangui, J.F. Doussin, N. Mattielli, South African dust contribution to the high southern latitudes and East Antarctica during interglacial stages, *Comm. Earth Environ*., 2022, **3**, 129, https://doi.org/10.1038/s43247-022-00464-z

(73) A. Jarošíková, V. Ettler, M. Mihaljevič, V. Penížek, T. Matoušek, A. Culka, P. Drahota, Transformation of arsenic-rich copper smelter flue dust in contrasting soils: A 2-yer field experiment, *Environ. Pollut.*, 2018b, **237**, 83-92, https://doi.org/10.1016/j.envpol.2018.02.028

(74) J. Csavina, A. Landázuri, A. Wonaschütz, K. Rine, P. Rheinheimer, B. Barbaris, W. Conant, A.E. Sáez, E.A. Betterton, Metal and metalloid contaminants in atmospheric aerosols from mining operations, *Water Air Soil Pollut.*, 2011, **221**, 145–157, https://doi.org/10.1007/s11270-011-0777-x

(75) A.M. Lopez, C.C.E. Avila, J.P. VanderRoest, H.K. Roth, S. Fendorf, T. Borch, Molecular insights and impacts of wildfire-induced soil chemical changes. *Nat. Rev. Earth Environ*., 2024, **5**, 431-446, https://doi.org/10.1038/s43017-024-00548-8

(76) S.G. Johnston, N. Karimian, E.D. Burton, Fire promotes arsenic mobilization and rapid arsenic(III) formation in soil via thermal alteration of arsenic-bearing iron oxides, *Front. Earth Sci.*, 2019, **7**, 139, https://doi.org/10.3389/feart.2019.00139

View Article Online
DOI: 10.1039/D6VA00064A

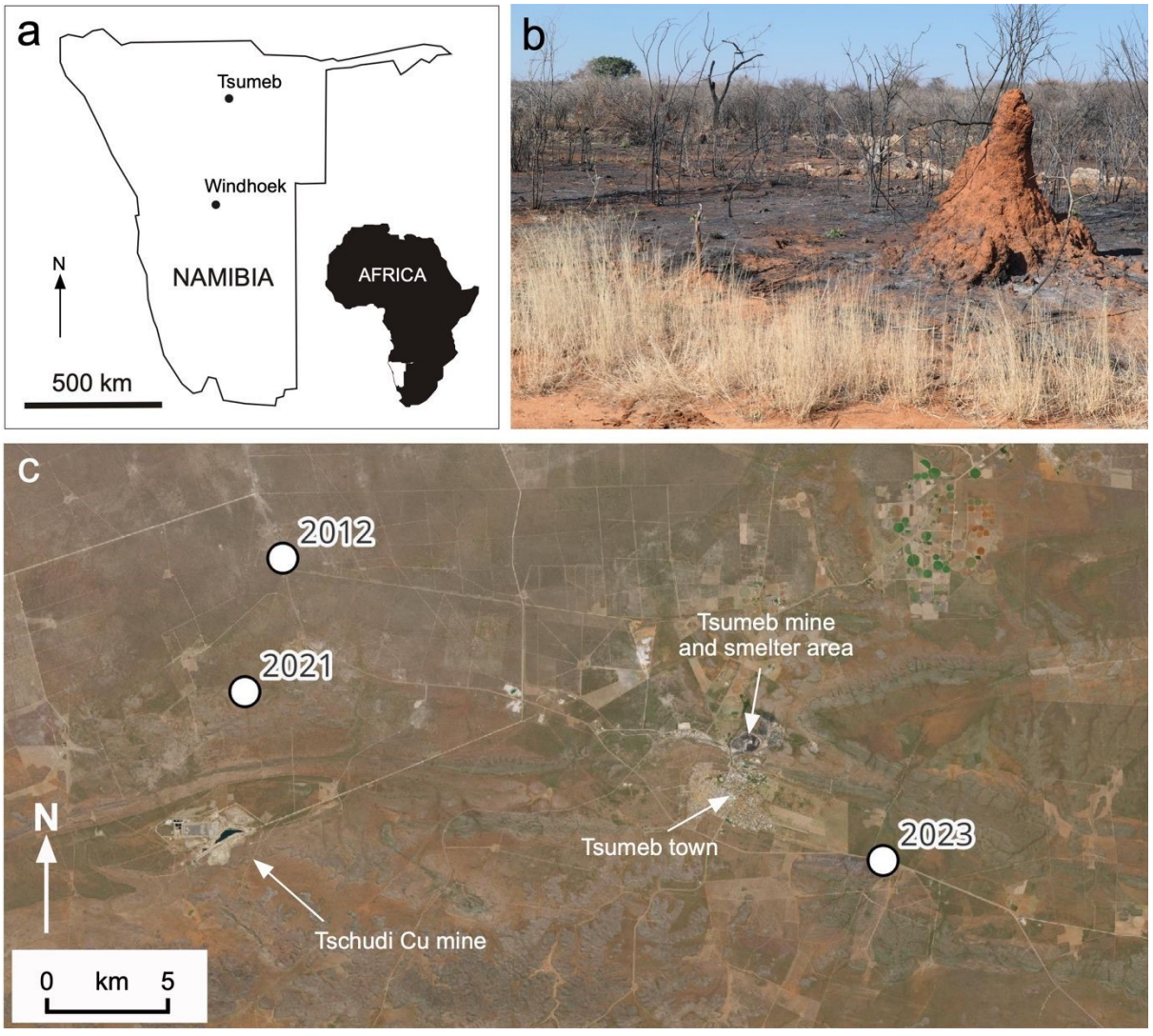

View Article Online
DOI: 10.1039/D6VA00064A

Figure 1. Location of the Tsumeb area (a), photograph of a burned area in 2023 (b), and a satellite photograph (based on Sentinel-2) of the soil sampling sites indicating the nearby mining and metallurgical sites.

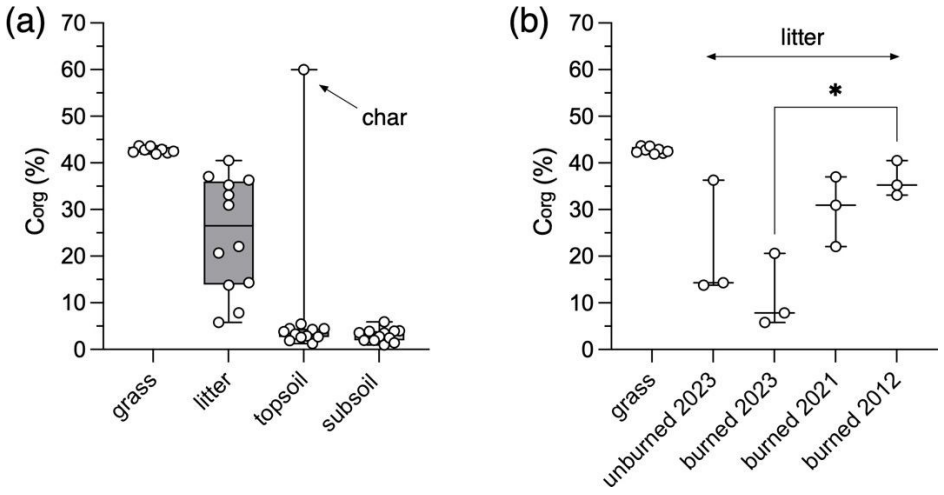

Figure 2. Organic carbon concentrations in the samples from the unburned and burned areas. (a) The C_{org} levels in the grass, litter, topsoil, and subsoil samples in the whole dataset indicating the largest variability in the litter (one-way ANOVA and Tukey's multiple comparison test suggests that the differences are statistically significant with a P-value < 0.004 except the difference between the topsoil and subsoil); (b) Changes in the C_{org} concentrations in the litter samples as a function of the year of the fire event (statistically significant difference indicated by * corresponds to a P-value ≤ 0.05 based on the one-way ANOVA and Tukey's multiple comparison test at alpha = 0.05).

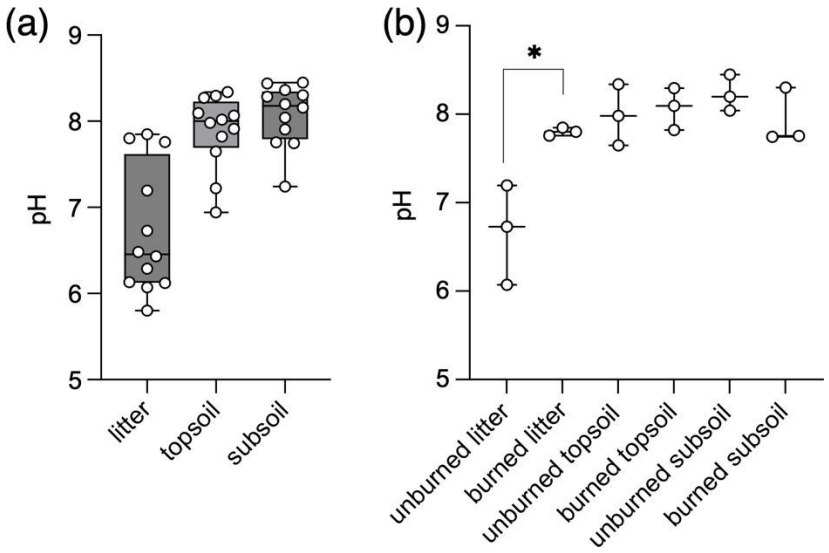

Figure 3. The pH variability in litter, topsoils, and subsoils. (a) Boxplot showing the differences in pH values of litter, topsoil, and subsoil samples (for the whole dataset); (b) A comparison of pH values for litter, topsoil, and subsoil from unburned and burned plots of the 2023 fire event (horizontal lines represent medians). A statistically significant increase in pH between unburned litter and burned litter (ash) was confirmed (one-way ANOVA, Tukey's multiple comparison test at alpha = 0.05).

View Article Online
DOI: 10.1039/D6VA00064A

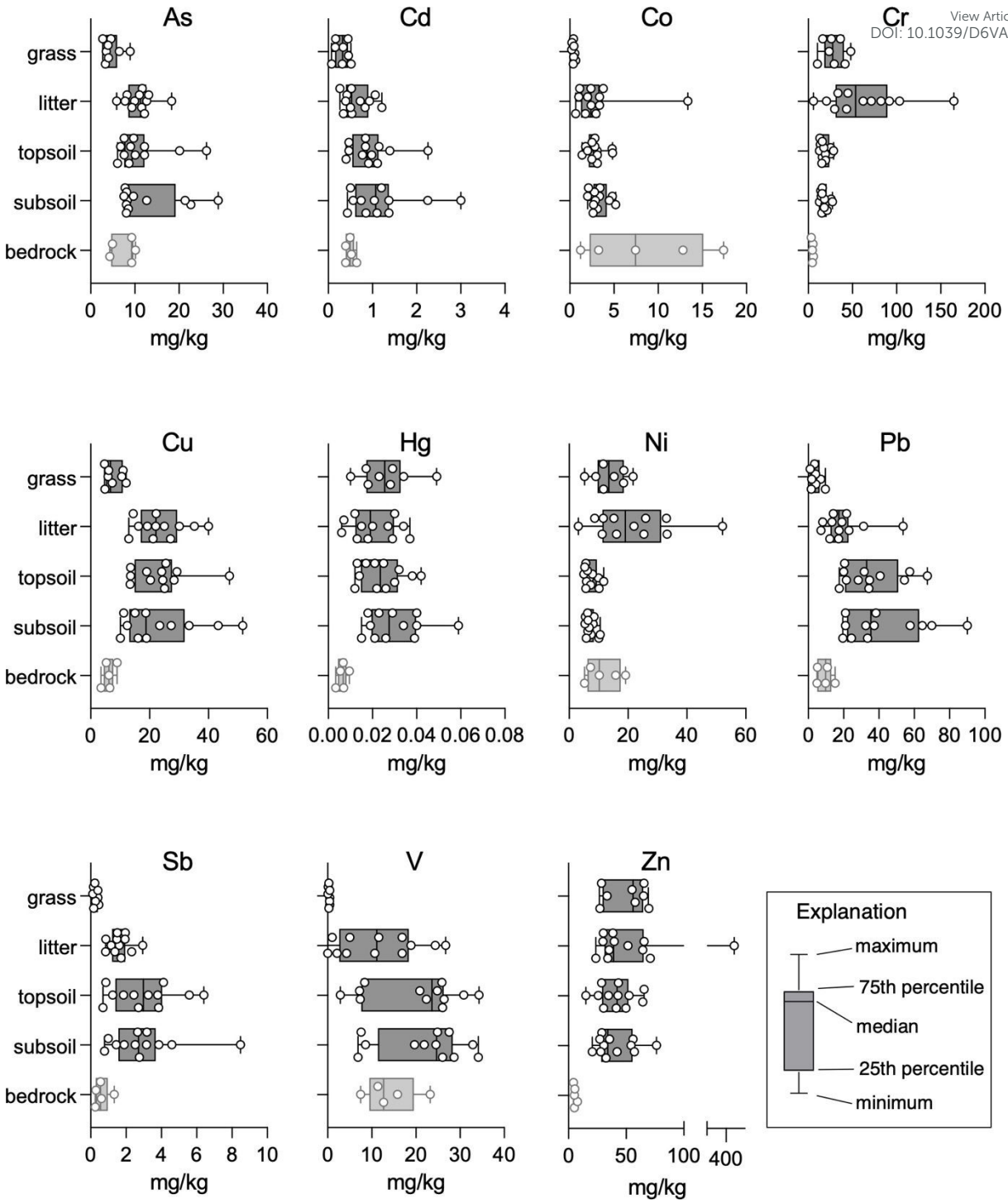

Figure 4. Variability of the concentrations of the trace elements (As, Cd, Co, Cr, Cu, Hg, Ni, Pb, Sb, V, and Zn) in the grass, surface soil layers, and bedrock (plotted for the entire dataset).

View Article Online
DOI: 10.1039/D6VA00064A

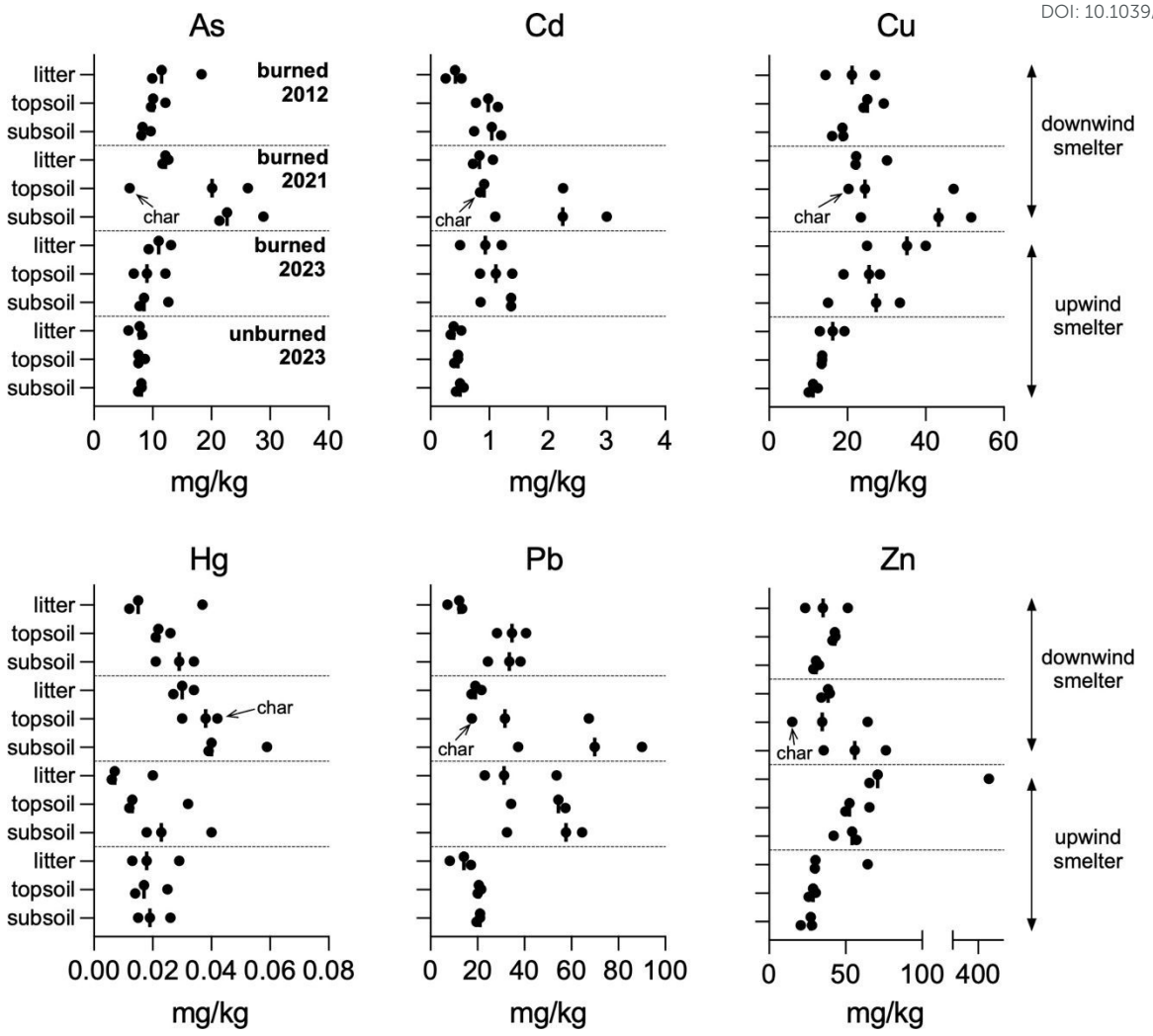

Figure 5. Site-specific concentration profiles showing the variability of the main smelter-derived pollutants (As, Cd, Cu, Hg, Pb, and Zn) at the litter-topsoil-subsoil interface (vertical lines correspond to median values). Sites burned in 2012 and 2021, and located downwind of the Tsumeb smelter, generally show an enrichment in most of the studied trace elements.

View Article Online
DOI: 10.1039/D6VA00064A

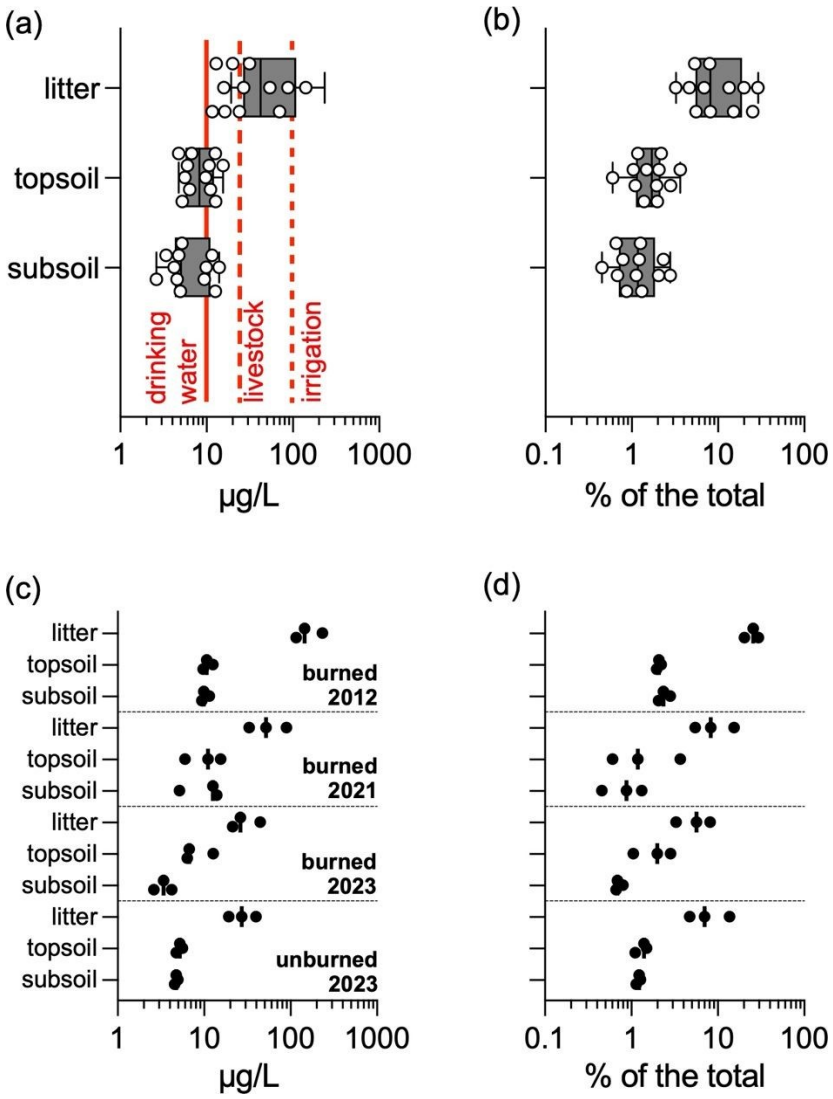

Figure 6. Arsenic concentrations in the water extracts (µg/L) and extractability (in % of the total) for the litter, topsoil, and subsoil samples, and comparisons with WHO's drinking water limits[65] and the CCME limits for water quality guidelines for livestock and irrigation.[62] Boxplots (a) and (b) correspond to the entire dataset, and plots (c) and (d) correspond to site-specific data.

View Article Online
DOI: 10.1039/D6VA00064A

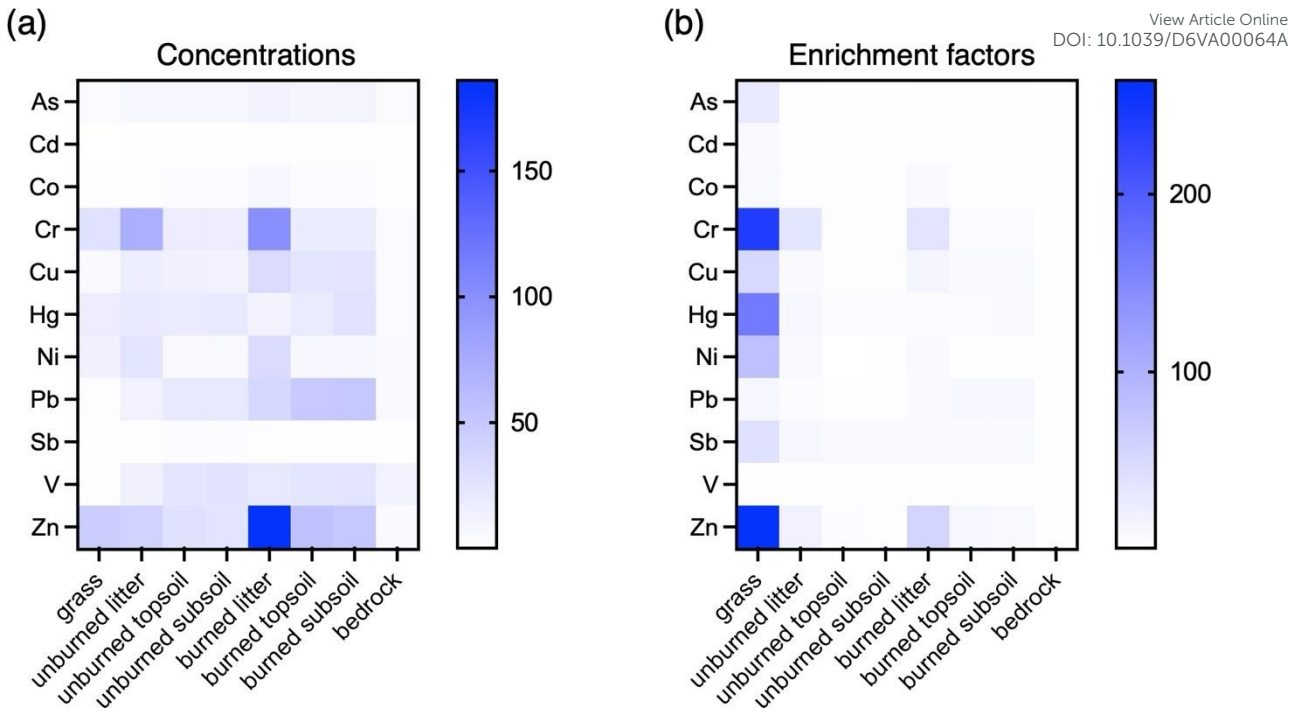

Figure 7. Heatmaps showing the changes in (a) the trace element concentrations (in mg/kg, except for Hg, which is expressed in µg/kg) and (b) enrichment factors (based on Me/Ti molar ratios) for the individual trace elements in the unburned and burned samples from the 2023 fire event. Two-way ANOVA and Tukey's multiple comparison test at alpha = 0.05 indicated that when the concentrations in the grass and bedrock are excluded from the calculations, the differences between the unburned and burned plots are statistically significant for the litter only in the case of Zn and the Zn/Ti molar ratio.

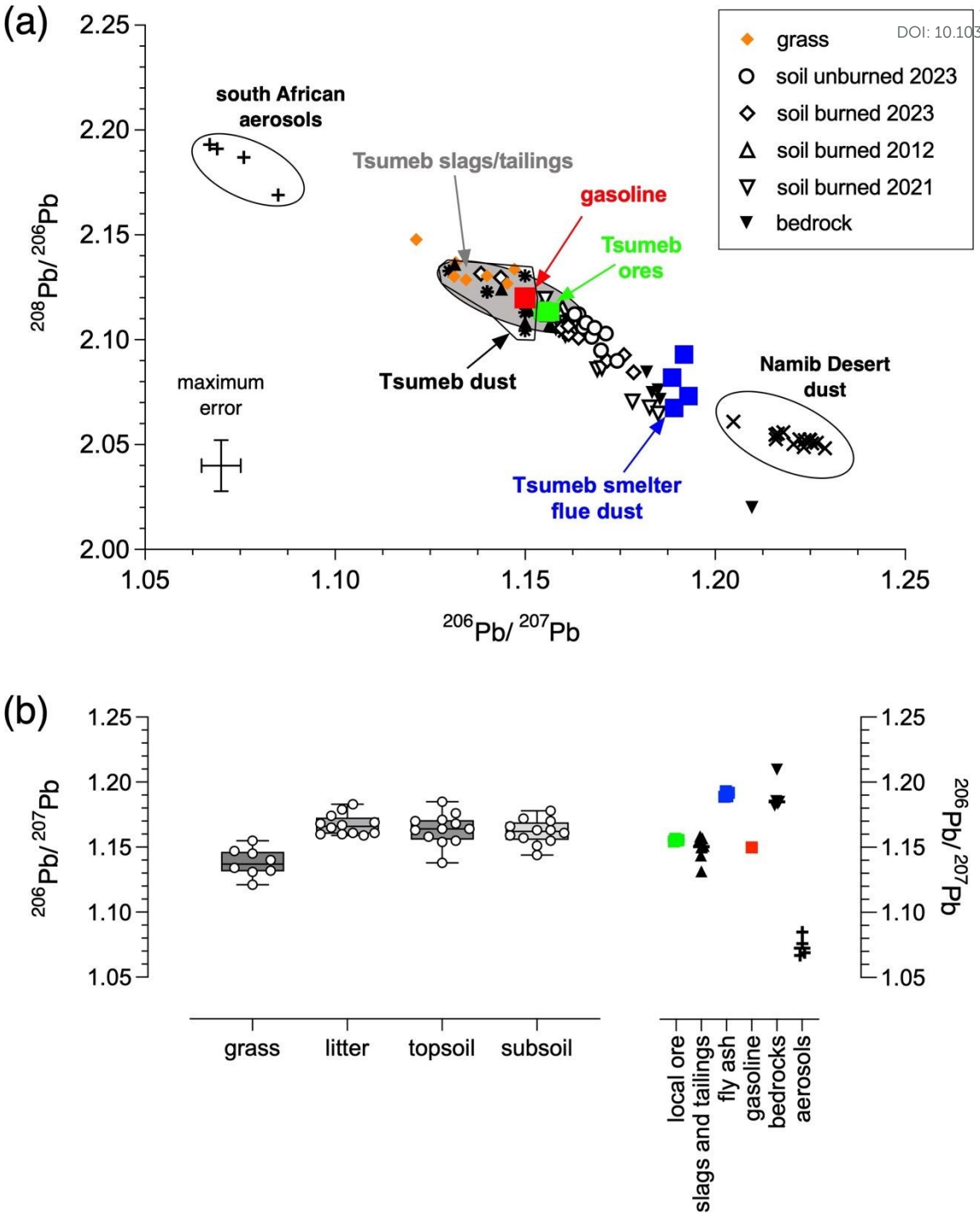

Figure 8. Lead isotopic data for the samples from the burned and unburned areas in the Tsumeb mining district, Namibia. (a) Three-isotope graph ($^{206}Pb/^{207}Pb$ versus $^{208}Pb/^{206}Pb$) showing the Pb isotopic composition of the grass and soils from the unburned and burned areas together with the potential Pb sources (gasoline, slags and tailings[46], Tsumeb dust[70], local ore[38], south African aerosols[71], Namib Desert dust Huab site[72], bedrock and recent smelter flue dust from this study); (b) Boxplot diagram showing the comparison of the $^{206}Pb/^{207}Pb$ values for the grass, litter, topsoil and subsoil from all the studied plots potential Pb sources.

Table 1. Basic statistics of the metal(loid)s concentrations in the grass, litter, topsoil, and subsoil from the burned and unburned areas in the Tsumeb area (Namibia) (in mg/kg, except for Hg). Reference values (median) from Tuhý et al.[20] (Hg) and Kříbek et al.[3] (other elements), and Canadian Soil Quality Guidelines[62] are reported for comparison purposes. Values in bold exceed the CCME guidelines for agricultural soils.[62] The complete dataset is available in the Supplementary Information (Table S4). NA – not available.

Element	**Grass** Range	Median	Mean	*Reference* Median	**Litter** Range	Median	Mean
As	2.70–8.95	3.97	4.69	*1.2*	5.88–**18.3**	11.2	11.0
Cd	0.07–0.51	0.32	0.30	*0.24*	0.26–1.21	0.52	0.64
Co	0.20–0.67	0.42	0.42	*NA*	0.65–13.4	2.40	3.18
Cr	10.4–48.2	27.7	29.0	*NA*	5.9–**165**	53.5	62.9
Cu	4.67–12.0	6.73	7.79	*4.35*	12.9–40.0	22.2	23.8
Hg (µg/kg)	10.1–48.7	25.2	25.8	*22.4*	5.57–36.7	19.5	20.6
Ni	5.24–21.7	13.5	13.9	*NA*	3.14–52.1	19.1	21.5
Pb	1.12–9.70	3.83	4.19	*2.03*	7.24–53.7	17.3	19.9
Sb	0.12–0.45	0.25	0.28	*NA*	0.84–2.94	1.56	1.64
V	0.09–0.47	0.35	0.33	*NA*	0.04–26.7	11.2	11.5
Zn	26.7–69.2	55.9	49.8	*30.2*	23.8–**421**	39.0	75.4

Element	**Topsoil** Range	Median	Mean	*Reference* Median	**Subsoil** Range	Median	Mean	*Reference* Median	*CCME Soil Guidelines* *Agricultural*	*Residential*
As	6.09–**26.2**	9.39	11.3	*28.4*	7.52–**28.9**	8.40	**12.6**	*3.4*	*12*	*12*
Cd	0.40–**2.26**	0.88	0.97	*4.1*	0.43–**3.00**	1.07	1.20	*0.3*	*1.4*	*10*
Co	1.40–4.83	2.84	2.90	*NA*	2.00–5.19	3.01	3.29	*NA*	*40*	*50*
Cr	12.5–28.7	16.8	18.6	*NA*	12.6–27.4	17.0	18.2	*NA*	*64*	*64*
Cu	13.4–47.1	24.3	23.6	*85*	10.1–51.6	18.8	23.4	*27*	*63*	*63*
Hg (µg/kg)	11.5–42.4	23.9	24.5	*68.3*	15.0–58.9	27.8	30.2	*NA*	*6600*	*6600*
Ni	5.02–11.7	6.55	7.30	*NA*	5.38–10.6	6.60	7.27	*NA*	*45*	*45*
Pb	17.5–67.4	33.0	35.7	*181*	19.6–90.0	35.4	42.5	*46*	*61*	*61*
Sb	0.70–6.40	2.98	3.07	*NA*	0.78–8.48	2.71	3.03	*NA*	*20*	*20*
V	2.88–34.3	23.6	19.8	*NA*	6.86–34.1	24.7	21.9	*NA*	*130*	*130*
Zn	15.0–65.5	42.1	41.2	*97*	20.7–76.2	34.1	40.8	*25*	*250*	*250*

View Article Online
DOI: 10.1039/D6VA00064A

Data Availability Statement

The data for this article are included as part of the Supplementary Information and are also available at Zenodo at https://doi.org/10.5281/zenodo.18497577.